SOILS, SEC 5 • SOIL LANDSCAPE AND ECOLOGY • RESEARCH ARTICLE

A phototrophy-driven microbial food web in a rice soil

Youzhi Feng · Xiangui Lin · Jianguo Zhu · Zhongjun Jia

Abstract

Purpose Light is a major driver of primary productivity in most ecosystems on Earth. Phototrophic microorganisms harvest light to synthesize organic biomass for sustaining the global energy and carbon flow. However, the bottom-up model of phototrophic microorganisms as primary production and food source for higher trophic levels remains unclear in the terrestrial environment.

Materials and methods Rice soil microcosms treated with different carbon sources (^{13}C-formate, ^{12}C-formate, or a control without formate) were incubated for 21 days under illumination. For each microcosm, genomic DNA were extracted and fractionated by isopycnic ultracentrifugation. Subsequently, the analyses were conducted on these samples with real-time quantitative PCR, PCR-denaturant gradient gel electrophoresis fingerprinting, and sequencing analysis of bacterial 16S rRNA, eukaryotic 18S rRNA, and photosynthetic functional genes.

Results and discussion Our analysis indicated that formate carbon was assimilated by a subset of bacteria and eukaryotes. Based on molecular fingerprinting and sequencing analysis, the primary producers were determined to be the microorganisms affiliated with purple phototrophic bacteria, cyanobacteria, and algae. The detection of protozoa and fungi-like 18S rRNA gene sequences in the ^{13}C-enriched DNA fractions suggested that these organisms acted as consumers. They fed on nutrients derived from labeled phototrophic microorganisms.

Conclusions Molecular evidence suggests that in the light-driven microbial food web, the carbon flow from formate is initiated by phototrophic primary and secondary producers. Their biomasses subsequently sustain the growth of consumers in the rice soil.

Keywords DNA-based stable isotope probing · Formate · Microbial food web · Phototrophy

Y. Feng · X. Lin (✉) · J. Zhu
State Key Laboratory of Soil and Sustainable Agriculture,
Institute of Soil Science, Chinese Academy of Sciences,
Nanjing 210008 Jiangsu Province, People's Republic of China
e-mail: xglin@issas.ac.cn

Z. Jia (✉)
Key Laboratory of Soil Environment and Pollution Remediation,
Institute of Soil Science, Chinese Academy of Sciences,
Nanjing 210008 Jiangsu Province, People's Republic of China
e-mail: jia@issas.ac.cn

1 Introduction

Phototrophy of microorganisms is an important process on Earth since it contributes significantly to the global carbon cycle (Field et al. 1998). Each year phototrophic prokaryotes provide more than 35.2% of global primary production in marine environments (Overmann and Garcia-Pichel 2006). Therefore, the phototrophy-based microbial food web plays an essential role in the sustainability of both energy and carbon flow in the environment (Tittel et al. 2003). However, little is known about this food web at the molecular level in past decades, particularly for soil environments (Moran and Miller 2007).

Light irradiation usually can reach the eutrophic zones of topsoil layer in a paddy field (Liesack et al. 2000). A phototrophy-based microbial food web is believed to sustain the cycles of nutrients and energy in terrestrial

environment (Al-Najjar et al. 2010). Figure 1 sketches such a microbial food web. Phototrophic microorganisms utilize light energy and assimilate organic and/or inorganic carbon for growth. The increase of biomass via phototrophic microorganisms is accompanied by an active growth of primary consumers in the microbial loop. At the same time, phototrophic microorganisms and primary consumers provide cell debris and exopolymeric substances that detritivorous fungi utilize. A bottom-up model of microbial food web in the rice soil can be built from carbon sources, primary producers, and consumers. However, there is no unambiguous evidence to identify microorganisms that drive the turnover and the transformation of organic materials in soil.

In DNA-based stable isotope probing (DNA-SIP), microorganisms grow on the ^{13}C-labeled substrate. The ^{13}C-carbon is incorporated into their biomass including DNA. After the isopycnic ultracentrifugation following DNA extraction, the ^{13}C-DNA produced during an active growth of metabolically distinct microbial groups is resolved from those of unlabeled members. Subsequent analysis can help to identify the microorganisms that are actively involved in a defined process. Therefore, DNA-SIP is extremely helpful to link the metabolic function and taxonomic identity of microorganisms involved in a defined ecological process (Radajewski et al. 2003). For example, this technology has been applied to track carbon flows due to methane-derived carbon (Deines et al. 2007;

Murase and Frenzel 2007) and organic matter decomposition (Lueders et al. 2006; Chauhan et al. 2009) in microbial food webs.

In this study, we have investigated the phototrophy-driven microbial food web in a paddy soil by using formate as the carbon source. There are three reasons for such a choice. First, formate is a ubiquitous major intermediate and fermentation product during organic decomposition in an anoxic environment (Kimura 2000; Penning and Conrad 2006). Second, formate is directly or indirectly involved in the growth of prokaryotic and eukaryotic organisms (Haddock and Ferry 1989; Baziramakenga et al. 1995). Finally, phototrophic microorganism growth is mostly stimulated by formate (Supplementary Figs. S1 and S2), despite the fact that other organic acids, such as acetate and lactate, are generally more abundant than formate in the rice soil (Penning and Conrad 2006). With DNA-SIP, we have found that the microorganisms, phylogenetically highly related to cyanobacteria, algae, and purple phototrophic bacteria, assimilated formate carbon. Evidences suggest that these microorganisms also support the growth of higher trophic organisms such as protozoa and fungi-like ones in the rice soil. We propose that through such a microbial food web, nutrients in soils are maintained, and the energy flow for soil productivity is carried out.

2 Materials and methods

2.1 SIP microcosm

Soil samples were taken from a rice–wheat rotation paddy field at China FACE station, Jiangsu Province, China (31° 35′ N, 120°30′ E). Soil physical and chemical properties were described in the supplementary information. Each SIP microcosm contained 5 g bulk soil and 0.5 mmol of ^{13}C-labeled formate (Kalyuzhnaya et al. 2008). The labeled formate was purchased from Sigma-Aldrich with 99 at.% ^{13}C. Two control microcosms were established for comparison. One was with ^{12}C-formate addition, and the other was without formate addition. All the incubations were performed with 120 ml serum bottle for 21 days at 30°C. One subset of samples was kept under continuous incandescent illumination with a light intensity of about 2,000 lx, while another subset was kept in darkness. Before incubation, the headspace of the serum bottle was repeatedly purged with N_2 to make the microcosm anaerobic. All treatments were carried out in duplicate.

Gas samples were taken with a gas-tight syringe from the headspace of the soil microcosms every 7 days. Production of CO_2 was monitored by a GC equipped with flame ionization detector as previously described (Ding et al. 2007).
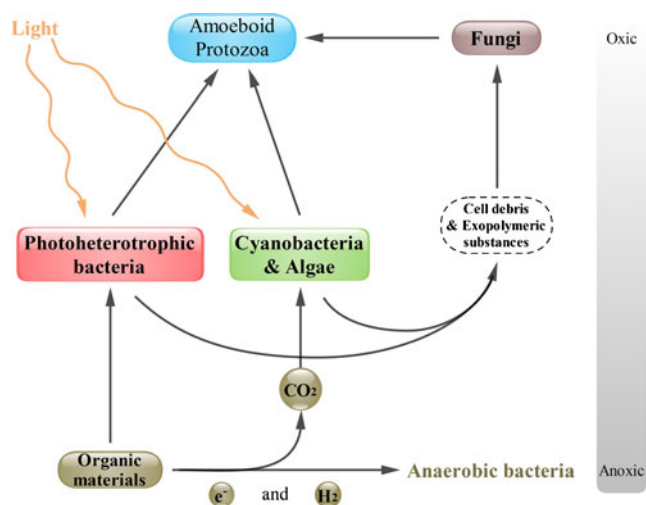
Fig. 1 A conceptual model for a phototrophy-driven microbial food web in a rice soil. Under anoxic conditions, organic materials are converted to CO_2, which fuels the growth of primary producers of cyanobacteria and algae. The light energy is also harvested by photoheterotrophic bacteria to metabolize organic materials directly as secondary producers. Amoeboid protozoa prey on the biomass of fungi and phototrophic microorganisms. Fungi likely assimilate the nutrients from cell debris and extracellular substance for growth. This microbial interaction constitutes the core set of nutrient and energy flow of the rice soil tested and maintains the soil productivity

2.2 DNA extraction and SIP gradient fractionation

On the day after final gas sampling, soil samples from each treatment were collected, mixed, and sieved (<2 mm). Samples were kept at −20°C for molecular analysis. A day after sampling, soil DNA was extracted using 0.5 g soil for each sample using a FastDNA® SPIN Kit for soil (MP Biomedicals, Santa Ana, CA, USA) according to the manufacturer's instructions. The extracted soil DNA was eluted in 50 μl TE buffer, quantified by spectrophotometer, and stored at −20°C before use.

Stable isotope probing fractionation was conducted in a similar manner as described by Jia and Conrad (2009) and Neufeld et al. (2007). Briefly, the gradient fractionation of total DNA extract (3.0 μg) from each SIP microcosm under illumination was performed with an initial CsCl buoyant density of 1.720 g/ml subjected to centrifugation at 177,000×g for 44 h at 20°C. The density gradient was aliquoted to 340 μl fractions, and the buoyant density of each fraction was determined by the refractive index. Fifteen fractions were generated covering buoyant densities from 1.696 to 1.743 g/ml, and nucleic acids were separated from CsCl by PEG 6000 precipitation and dissolved in 30 μl TE buffer.

2.3 Real-time quantitative PCR of purple phototrophic bacterial *pufM* genes, bacterial 16S rRNA genes, and eukaryotic 18S rRNA genes

Copy numbers of *pufM* gene fragment in the each fractionated DNA gradient were quantified by real-time quantitative PCR (qPCR), using primer set *pufM*557F/*pufM*750R (Table 1). qPCR was also performed for both bacterial 16S rRNA gene and eukaryotic 18S rRNA gene abundances by using primer sets 519F/907R and Euk1A/Euk516R (see Table 1) for all treatments. The detailed description for qPCR was shown in supplementary information.

2.4 Denaturant gradient gel electrophoresis analysis of bacterial 16S rRNA and eukaryotic 18S rRNA gene sequences

The community compositions of bacteria and eukaryotes in each fractionated DNA gradient were characterized by PCR-denaturant gradient gel electrophoresis (DGGE) fingerprinting analysis with the primer sets of 341F-GC/907R and Euk1A/Euk516R-GC (see Table 1). Both bacterial 16S rRNA and eukaryotic 18S rRNA genes PCR products were separated on 6% (*w/v*) polyacrylamide gels with a 30–70% denaturing gradient (urea and formamide). DGGE gels were run at a constant voltage of 85 V for 16 h at 60°C in 1× TAE buffer (40 mM Tris, 20 mM acetic acid, 1 mM EDTA; pH 8.3) and subsequently stained in 1:10,000 SYBR Green I and scanned with Gel Doc™ EQ imager combined with

Quantity one 4.4.0 (Bio-Rad). The representative bands were excised, left overnight in 25 μl Milli-Q water, reamplified, and run again on the DGGE system to ensure purity and correct mobility of the excised DGGE bands. Correct PCR products were purified using the QIAquick PCR Purification kit (QIAGEN) before cloning.

2.5 Cloning, sequencing, and phylogenetic analysis

The purified PCR amplicons of the excised DGGE bands were cloned into a pMD18-T vector (TaKaRa) and transformed into *Escherichia coli* DH5α competent cell. Six random clones containing correct gene size for each DGGE band were sequenced by Invitrogen Sequencing Department in Shanghai. DNASTAR software package was used to manually check and compare the clone sequences. One representative clone sequence with high quality after sequence comparison from each band was used for phylogenetic analysis. Together with the top three BLAST hits of homologous gene sequences, the DGGE band sequences were used to build a basic phylogenetic tree by the neighbor-joining method using the software package of Molecular Evolutionary Genetics Analysis 4.0 version (Tamura et al. 2007). The tree topology was further evaluated by different methods including minimum evolution and maximum parsimony. The phylogenetic relationships of 16S rRNA gene or 18S rRNA gene sequences to the closest homolog in the GenBank were then inferred. The GenBank accession numbers for the 16S rRNA and 18S rRNA gene fragments sequenced in this study are AB525842 to AB525862 and AB526173 to AB526195, respectively.

2.6 Statistical analysis

DNA fingerprints obtained from the 16S to 18S rRNA gene banding patterns on the DGGE gels were photographed and digitized using Bio-Rad's Quantity One software. Using the digital matrix obtained from DGGE, the similarities (or dissimilarities) among genotypes from the DNA fractionations could be quantified using cluster analysis. Euclidean distances were calculated from relative positions and intensities of bands, and the samples were clustered using Pearson's product-moment coefficient and an unweighted pair group method with arithmetic mean (UPGMA) algorithm.

3 Results

3.1 Microbial CO_2 evolution in the DNA-SIP microcosm

CO_2 concentrations were monitored to assess the microbial activity during the 21-day incubation period. With formate treatment, the CO_2 concentration reached a maximum of

Table 1 Primers used in this study

Target	Forward primer	Reverse primer	Length (bp)[b]	Usage	Reference
Bacterial 16S rRNA genes	341F-GC[a] (CCTACG GGAGGCAGCAG)	907R (CCGTCAATT CMTTTRAGTTT)	560	DGGE	Muyzer et al. (1998)
	519F (CAGCMGCC GCGGTAATWC)	907R	400	qPCR	Biddle et al. (2008)
Eukaryotic 18S rRNA genes	Euk1A (CTGGTTG ATCCTGCCAG)	Euk516R-GC[a] (ACCA GACTTGCCCTCC)	560	DGGE and qPCR	Beatriz et al. (2001)
All *pufM* genes	*puf*LF (CTKTTCGA CTTCTGGGTSGG)	*pufM*750R (CCCATG GTCCAGCGCCAGAA)	1,500	Agarose gel electrophoresis	Nagashima et al. (1997)
	*pufM*557F (CGCAC CTGGACTGGAC)	*pufM*750R	229	qPCR	Achenbach et al. (2001)

[a] Indicates a GC clamp that was added to the 5′ end of the primer for DGGE fingerprinting analysis as described

[b] PCR product length in base pairs

around 45–55 µmol/g d.w.s on the 14th day and started to decline afterward for the illuminated samples (Fig. 2). Comparatively, the CO_2 concentration was much lower in the control without formate addition, regardless of whether or not the sample was held in darkness. CO_2 reached a maximum of 15 µmol/g d.w.s on the 7th day and declined afterward under illumination. The reduction of CO_2 was possibly attributed to photoautotrophic growth of microorganisms such as green algae and cyanobacteria due to light stimulation (Supplementary Fig. S3). This was further supported by the fact that without illumination, CO_2 was
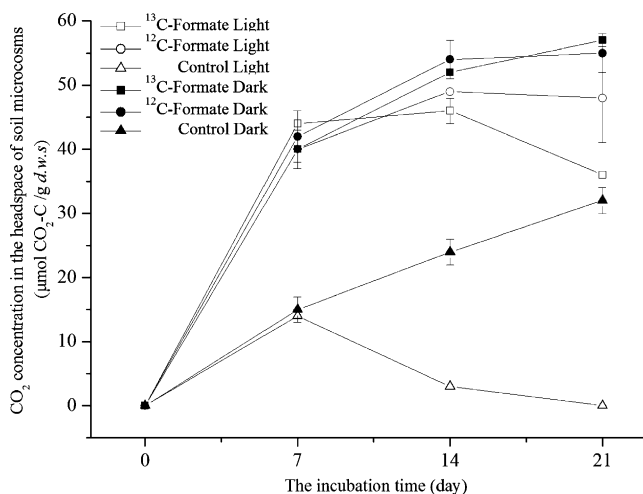

Fig. 2 CO_2 evolution in soil microcosms during incubation for 21 days. [13]C- and ^{12}C-formate denote the soil treated with [13]C- and ^{12}C-formate, respectively. The *light* and *dark* indicate the treatment under illumination and in darkness, respectively. Control denotes the treatment without formate addition. Standard error bars were obtained from two true replicates

continuously accumulated in the microcosms regardless of all treatments (see Fig. 2).

3.2 Quantitative analysis of genes in different DNA fractions by qPCR

With qPCR, we studied the purple phototrophic bacterial *pufM* gene abundance for different DNA gradients. Results clearly indicated that the labeled formate carbon was actively assimilated by *pufM* gene-containing microorganisms (Fig. 3a). The copy number of *pufM* gene peaked in the "heavy" DNA fractions (i.e., buoyant density 1.726, 1.728, 1.731, and 1.735 g/ml) for ^{13}C-formate-treated soil. In contrast, the highest copy number of *pufM* genes occurred in the "light" DNA fractions (i.e., buoyant density 1.720 and 1.722 g/ml) for ^{12}C-formate-treated soil (see Fig. 3a). Agarose gel electrophoresis of the near full length of *pufM* gene amplicons across the entire DNA gradients further supported this observation (Supplementary Fig. S4). When a sample was treated either without illumination or without formate addition, the copy number of *pufM* genes remained extremely low across the spectrum of different densities (see Fig. 3a). Interestingly, the majority of bacterial 16S rRNA genes were observed in the "heavy" DNA fractions (see Fig. 3b), implying *pufM* gene-containing phototrophic microorganisms likely dominated bacterial community in formate-treated soil under illumination. It is very interesting to notice that, compared to the bacterial 16S rRNA and purple phototrophic bacterial *pufM* genes, the eukaryotic 18S rRNA gene abundance in the "heavy" DNA fractions was much lower (see Fig. 3c). This phenomenon suggests that only a small fraction of
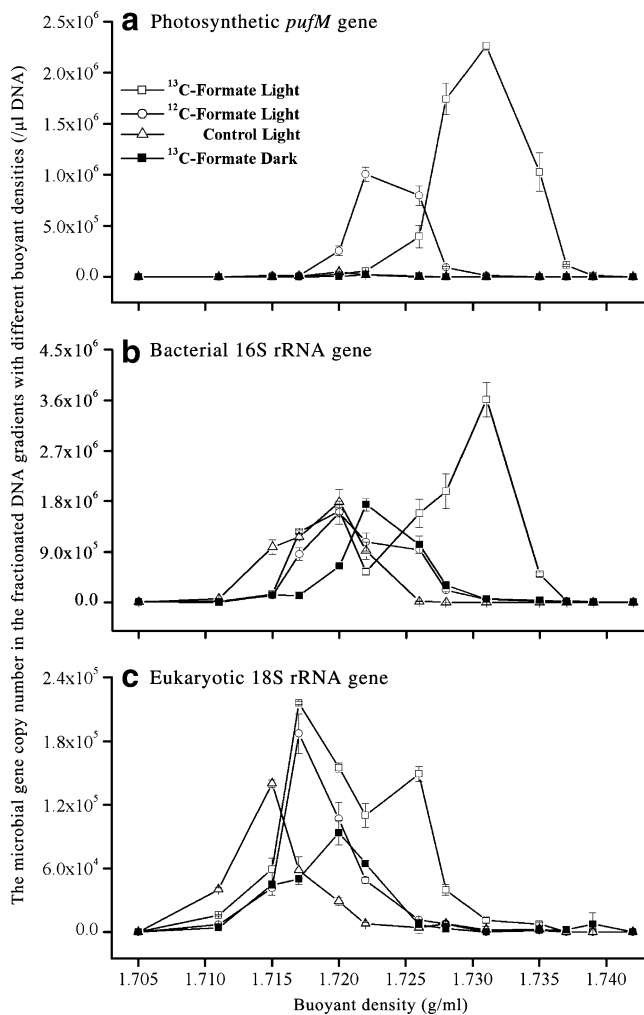
Fig. 3 Distributions of the copy number of photosynthetic *pufM* gene (**a**), bacterial 16S rRNA gene (**b**), and eukaryotic 18S rRNA gene (**c**) across the buoyant densities of the DNA gradients isolated from soil samples treated with ^{13}C-, ^{12}C-formate, or control under illumination or in darkness. All other designations are the same as those in Fig. 2

eukaryotic community actively assimilated formate-derived carbon in the ^{13}C-formate-treated soil under illumination.

3.3 Soil bacteria actively involved in the phototrophy-based microbial food web

The phylogenetic identity of bacteria involved in the metabolism of formate-derived carbon under illumination was analyzed by PCR-DGGE fingerprints (Fig. 4). A cluster analysis on the 16S rRNA gene fingerprint patterns revealed the differences between the "heavy" and "light" DNA fractions from soil samples treated with ^{13}C-formate and the differences between "light" DNA fractions from soil samples treated with formate and control (see Fig. 4b). At 0.48 Euclidean distance, the bacterial compositions in the "heavy" DNA fractions (i.e., buoyant density 1.726, 1.728, 1.731, and 1.735 g/ml) were grouped into one cluster

and separated from those in the "light" DNA fractions (see Fig. 4b), suggesting that several specific bacteria assimilated ^{13}C-formate and their nucleic acids became "heavier". The community in the "heavy" DNA fractions consisted of PCR-DGGE bands 8, 9, 11, 12, 16, and 21 (see Fig. 4a). Phylogenetic analysis revealed that the sequences of bands 8, 11, and 12 were highly related to the photoautotrophic cyanobacteria such as *Oscillatoria* (>90% sequence similarity), while bands 9, 16, and 21 were grouped with photoheterotrophic purple bacteria *Rhodopseudomonas* and *Rhodoplanes* (>70% sequence similarity; Fig. 5).

The bacterial community compositions from formate-treated soil samples are highly distinct from those without formate addition, as their fingerprint patterns were separated at 0.28 Euclidean distance (see Fig. 4b). Indeed, bands 13 and 18 found in the control disappeared when the bacterial community was treated with formate, while several other bands (such as 4 and 6) appeared (see Fig. 4a). Sequencing analysis indicated that they were closely related to uncultured *Nitrospirae* bacteria (band 13, 99% sequence similarity), *Rhodoplanes* (band 18, 96% sequence similarity), uncultured *Firmicutes* bacteria (band 4, 99% similarity), and *Alkaliphilus transvaalensis* (band 6, 98% sequence similarity), respectively (see Fig. 5).

3.4 Soil eukaryotes actively involved in the phototrophy-based microbial food web

Similar shifts in the eukaryotic communities were observed by the cluster analysis of 18S rRNA genes fingerprint patterns in the "heavy" and "light" DNA fractions. PCR-DGGE fingerprinting compositions in the "heavy" DNA fractions (i.e., buoyant density 1.721, 1.726, 1.728, and 1.731 g/ml) clustered in dendrogram (Fig. 6b). Their patterns are distinctly different from those in the "light" DNA fractions (see Fig. 6a), indicating that only a subset of the eukaryotic community assimilated ^{13}C-formate. Sequences of the bands retrieved in the "heavy" DNA fractions can be grouped with *Arachnula* (bands 8, 9, and 11, >95% sequence similarity), *Scenedesmaceae* (bands 12, 13, and 14, >95% sequence similarity), *Flamella arnhemensis* (band 16, 98% sequence similarity), and *Asterostroma* (band 17, 93% sequence similarity).

The eukaryotic communities in the control also clustered in a separate group (see Fig. 6b). For example, bands 20 to 23 only appeared in the control treatment (see Fig. 6a). Phylogenetic analysis revealed that these band sequences were highly related to those of *Crustacea* (bands 20, 21, and 23, >90% sequence similarity) and *Pithophora* sp. Kamigori (band 22, 96% sequence similarity; Fig. 7). The eukaryotic communities in the "light"
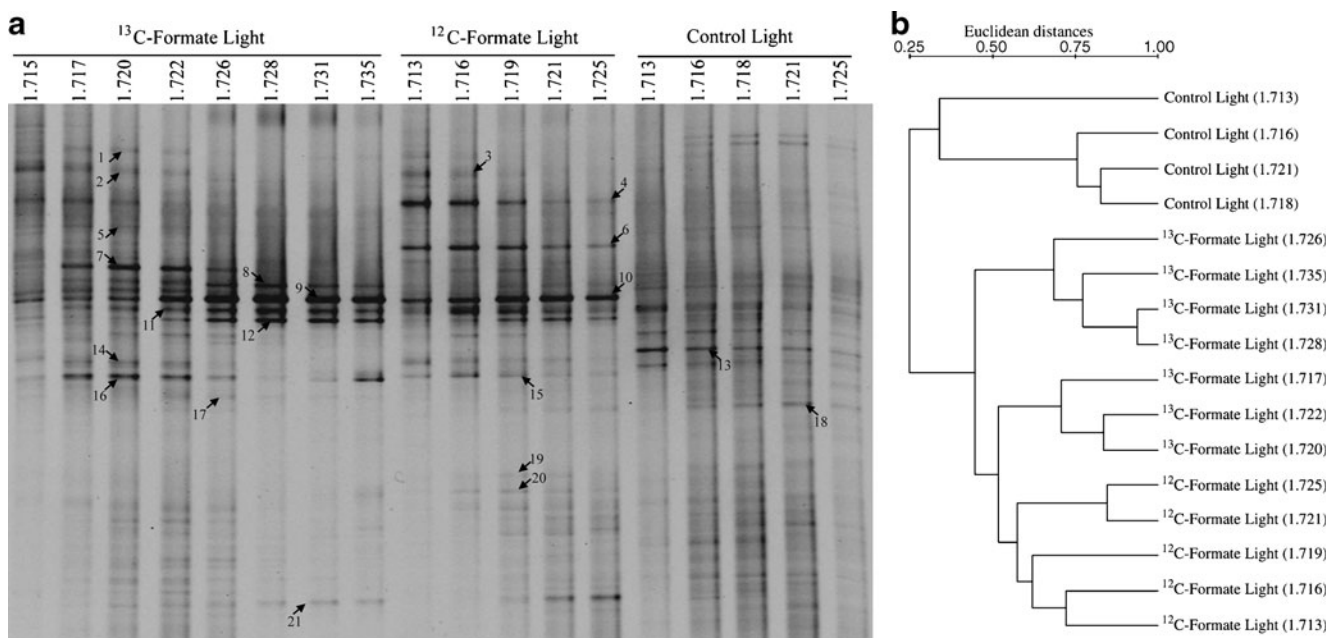
Fig. 4 PCR-DGGE fingerprinting profiles of bacterial 16S rRNA genes (**a**) and cluster analysis of PCR-DGGE band patterns (**b**) in the "heavy" and "light" DNA fractions from ^{13}C-, ^{12}C-formate, and control treatments under illumination. Above each DGGE lane is the buoyant density of the DNA used for PCR-DGGE analysis. Both "light" and "heavy" DNA fractions were analyzed for ^{13}C-formate treatment, while only the "light" fractions from ^{12}C-formate and control treatment were shown. The bands excised for sequencing analysis are indicated by *arrowed number* from *1* to *21*. The dendrogram of cluster analysis was produced by using Pearson's product-moment coefficient and a UPGMA clustering algorithm. Scale indicates Euclidean distance. All other designations are the same as those in Fig. 2

DNA fractions from ^{13}C- to ^{12}C-formate-treated soil samples were similar (see Fig. 6a), and they are categorized in one group (see Fig. 6b). Bands 2 to 7 invariably appeared in the "light" DNA fractions from the soils treated with formate (see Fig. 6a), and they were found to be affiliated with *Cercozoa* group (>80% sequence similarity; see Fig. 7).

### 3.5 A conceptual model for bottom-up control of microbial food web in a rice soil

Providing molecular evidences, DNA-SIP tracks the carbon flow through phototrophic microorganisms to higher trophic levels in a rice soil. Figure 1 sketches a conceptual bottom-up model of microbial food web based on these evidences. When stimulated by light, photoheterotrophic purple bacteria such as *Rhodopseudomonas* and *Rhodoplanes* directly metabolize formate, while photoautotrophic cyanobacteria *Oscillatoria* and algae *Scenedesmaceae* assimilate formate-derived CO_2. Concomitantly, oxygen generated by cyanobacteria and algae stimulates the growth of Amoebozoa *Arachnula*, *F. arnhemensis*, and fungi *Asterostroma*. These protozoa and fungi could grow on the biomass and/or metabolites of phototrophic microorganisms. Thus, a phototrophy-driven microbial food web forms in the rice soil.

4 Discussion

Light provides energy for phototrophic microorganisms and sustains the microbial food web. With molecular evidences provided by DNA-SIP, we propose a novel conceptual model (Fig. 1) for a phototrophy-driven food web in the rice soil. The model shows the bottom-up control of key microorganisms in this web. Phototrophic primary producers for maintaining the stability of complex microbial loop are identified, and their significances are highlighted in this proposed model.

In soil microcosms incubated with formate for 21 days, the microbial mat in red could be visualized under illumination (Supplementary Fig. S3a–d). The red and bright microbial consortium has been well recognized as anoxygenic purple phototrophic bacteria inhabiting anoxic environment and acting as secondary primary producer (Pfennig 1978). By analyzing the abundance distributions of purple phototrophic bacterial *pufM* gene (Fig. 3a and Supplementary Fig. S4) and bacterial 16S rRNA genes (see Fig. 3b) in fractionated DNA gradients, it is clear that purple phototrophic bacteria assimilated formate for growth. In addition, the active growth of purple phototrophic bacteria can also be safely inferred by finding an extremely low abundance of *pufM* genes in the "light" DNA fractions treated by ^{13}C-formate (see Fig. 3a). This

Fig. 5 Phylogenetic tree analysis showing the relationship of bacterial 16S rRNA genes of PCR-DGGE fingerprints in Fig. 4 to the closest relatives in the GenBank. Bootstrap values are indicated with support values as *circle* (50–70%), *square* (71–90%), and *triangle* (>90%). *Scale bar* indicates the number of nucleotide acid substitutions per site. All other designations are the same as those in Fig. 2
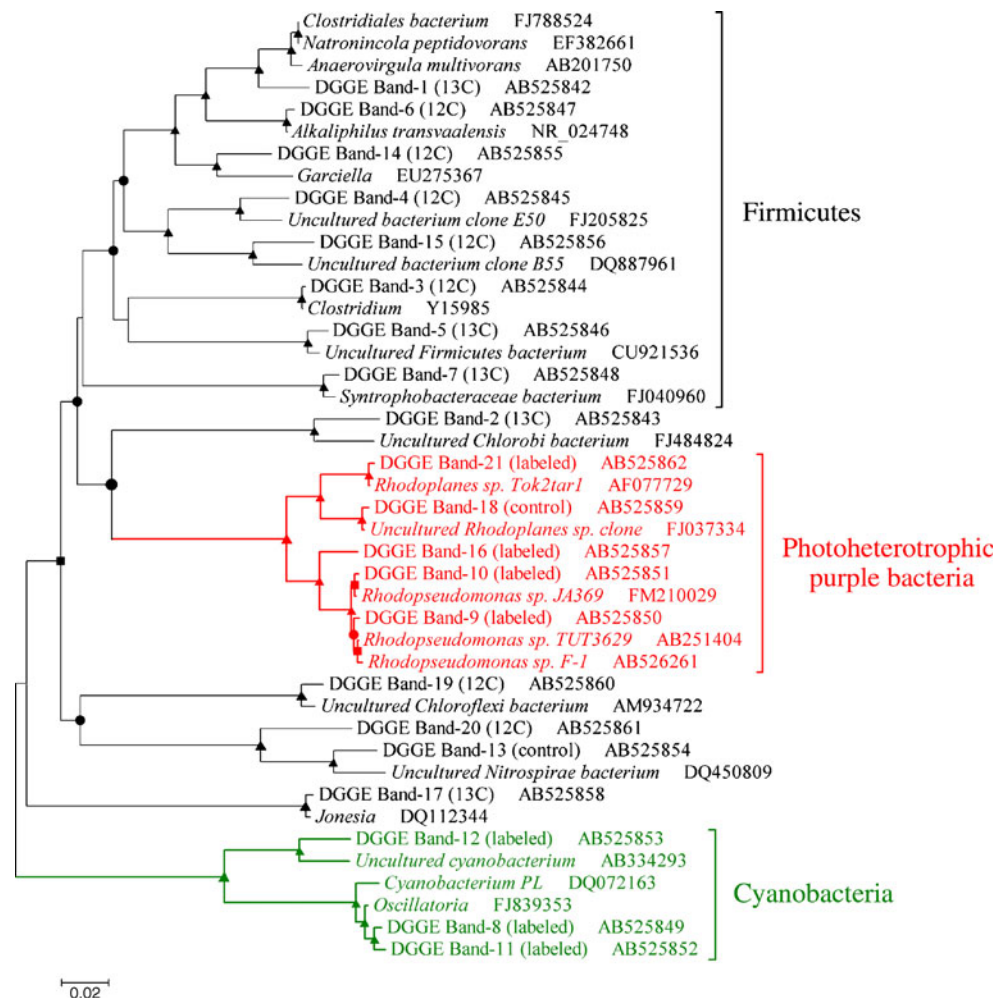

fact indicates that a large majority of the *pufM*-containing phototrophs had replicated at least once and acquired "heavy" DNA; those that had not replicated were not even detectable in the "light" DNA fractions. This observation agrees with the previous findings that in anoxic environment, purple phototrophic bacteria utilize light energy to assimilate small molecular weight organic compounds for growth (Imhoff 1988). Sequencing analysis of DGGE bands in the ^{13}C-DNA-labeled "heavy" fractions revealed that *Rhodopseudomonas* and *Rhodoplanes* assimilated ^{13}C-formate in soil (see Fig. 5).

Rhodopseudomonas and *Rhodoplanes* are typically photoheterotrophic purple non-sulfur bacteria in paddy soil (Harada et al. 2003; Lakshmi et al. 2009). Using culture-reliant approach, *Rhodopseudomonas* was indeed isolated and found to be the dominant purple phototrophic bacteria in rice soil tested in our previous work (Feng et al. 2009). The active growth of purple phototrophic bacteria was also widely observed in other anoxic environment (Madigan and Gest 1979; Overmann and Garcia-Pichel 2006). The widespread presence of *Rhodopseudomonas* and *Rhodoplanes* has suggested that they played an important role in sustaining

ecosystem productivity by driving the carbon and energy flows in anoxic and photic environment (Jiao et al. 2007).

Besides being a substrate to support the growth of photoheterotrophic purple bacteria, formate is an accessory reductant and electron donor for anaerobic bacteria, such as sulfate-reducing bacteria (Ferry 1990), which makes formate readily oxidized to CO_2. We observed a 3- to 4-fold increase of CO_2 accumulated in the microcosms treated with formate, compared to those without formate treatment (see Fig. 2). The $^{13}CO_2$ product by anaerobic formate oxidation could stimulate the growth of photoautotrophic organisms under illumination. DNA-SIP analysis on the "heavy" DNA fractions from labeled treatment indicates that ^{13}C-labelings of both cyanobacteria *Oscillatoria* (bands 8, 11, and 12 in Fig. 4a) and algae *Scenedesmus* (bands 12, 13, and 14 in Fig. 6a) were successful. Cyanobacteria *Oscillatoria* and algae *Scenedesmus* were found to be the dominant photoautotrophic microbes in paddy soil (Fujita and Nakahara 2006; Asari et al. 2008). With light stimulation, cyanobacteria and algae can live on CO_2 as the sole carbon source for growth and release O_2 (Overmann and Garcia-Pichel 2006). This photosynthetic activity
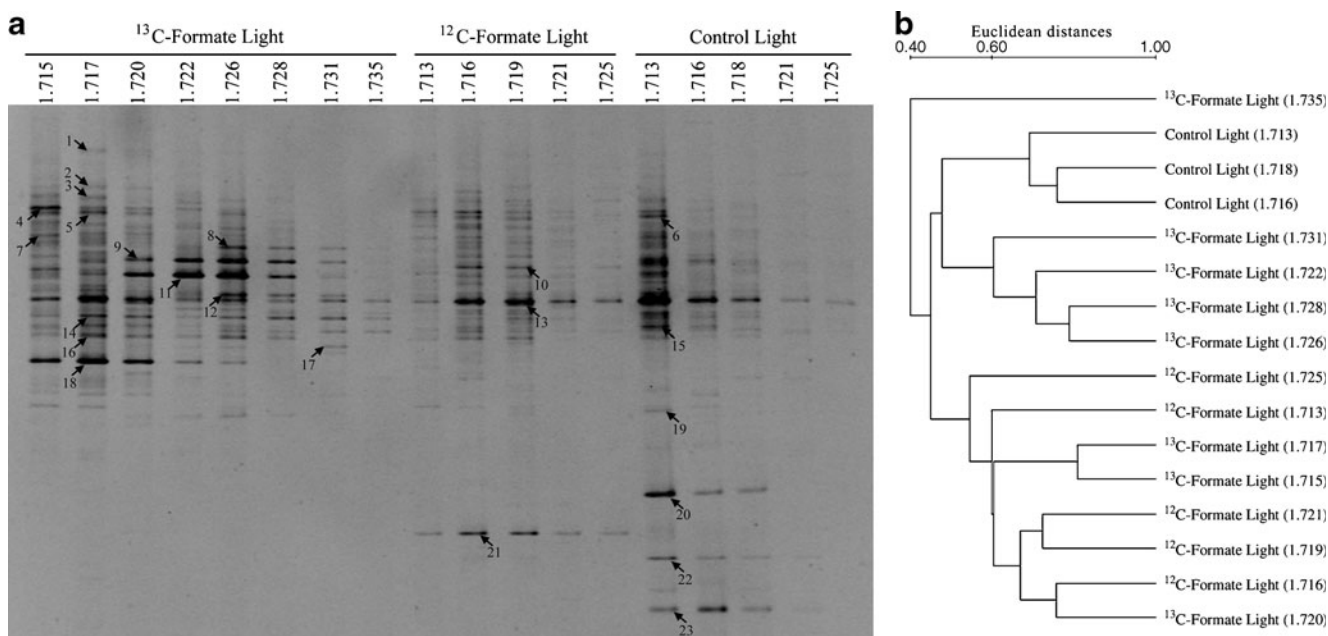
Fig. 6 PCR-DGGE fingerprinting profile of eukaryotic 18S rRNA genes (**a**) and cluster analysis of PCR-DGGE band patterns (**b**) in the "heavy" and "light" DNA fractions from ^{13}C-, ^{12}C-formate, and control treatments under illumination. The bands excised for sequencing analysis are indicated by *arrowed number* from *1* to *23*. All other designations are the same as those in Fig. 4

explains the decline in CO_2 accumulation in the headspace of soil microcosms under illumination (see Fig. 2). The concomitant production of O_2 leads to the phototrophic community shift from purple phototrophic bacteria to green cyanobacteria and algae (Supplementary Fig. S3b, d, and f). This observation agrees with the previous reports that *Rhodopseudomonas* sp. is succeeded by cyanobacteria in rice soil (Haque et al. 1969; Matsuguchi and Yoo 1981) and in artificial biofilm incubator under illumination (Roeselers et al. 2007). As a consequence, the proliferation of oxygenic photoautotrophic microorganisms could lead to niche differentiation from anoxic to oxic conditions, favoring the aerobically heterotrophic carbon utilization by higher trophic levels such as microflora and eukaryotes (Murase et al. 2006; Sugano et al. 2007).

With qPCR quantification (see Fig. 3c) and DGGE fingerprinting analysis (see Fig. 6a) on fractionated DNA gradients, we found that protozoa and fungi assimilate the formate-derived carbon, via directly or indirectly paths. The labeled protozoa were phylogenetically related to *Arachnula* (bands 8, 9, and 11) and *F. arnhemensis* (band 16) of Amoebozoa (see Fig. 7). The high intensity of DGGE bands suggests that *Arachnula*-like protozoa play a much more important role in the turnover of biomass from phototrophic microorganisms than *F. arnhemensis*-like protozoa (see Fig. 6a), although they are phylogenetically close to each other (Kudryavtsev et al. 2009). Meanwhile, aerobic growth of fungi was detected in the "heavy" DNA fractions, presumably a result of the increase in oxygen and

biomass released from cyanobacteria to algae. Fungi, bacteria, and algae all can be fed on by known *Arachnula* species (Bass et al. 2009). Therefore, *Arachnula* could be the key primary consumer within the phototrophy-based microbial food web in rice soil. Interestingly, reports of *Arachnula*-like protozoa in paddy soil are rare in the literature (Cahyani et al. 2004; Hatamoto et al. 2008). In addition, stable isotope probing of a methane-driven microbial food web indicated the absence of *Arachnula*-like protozoa in rice soils under dark conditions (Murase et al. 2006; Murase and Frenzel 2007). Therefore, we speculated that the *Arachnula* might constitute only a minor fraction of eukaryotic community in rice soil and was selectively stimulated by preying upon phototrophic microorganisms. Furthermore, such microbial interactions and trophic network could be habitat specific because of the habitat-specific predation on microbes by protozoa. In aquatic environment, amoeboid protozoa are often considered to be negligible predators in planktonic food webs (Callieri et al. 2002; Pickup et al. 2007). Up to 97% of carbon flux depended on flagellates and ciliates but not amoebae in a lake ecosystem (Callieri et al. 2002). In aerobic terrestrial environments, however, amoeboid protozoa might be essential players in the transfer of carbon and energy in the microbial food web (Murase et al. 2006; Murase and Frenzel 2007).

The predation relationship shapes the composition of microorganisms within the microbial food web (Tittel et al. 2003). The formate-based phototrophy leads to apparent

Fig. 7 Phylogenetic tree analysis showing the relationship of eukaryotic 18S rRNA genes of PCR-DGGE fingerprints in Fig. 6 to the closest relatives in the GenBank. All other designations are the same as those in Fig. 5
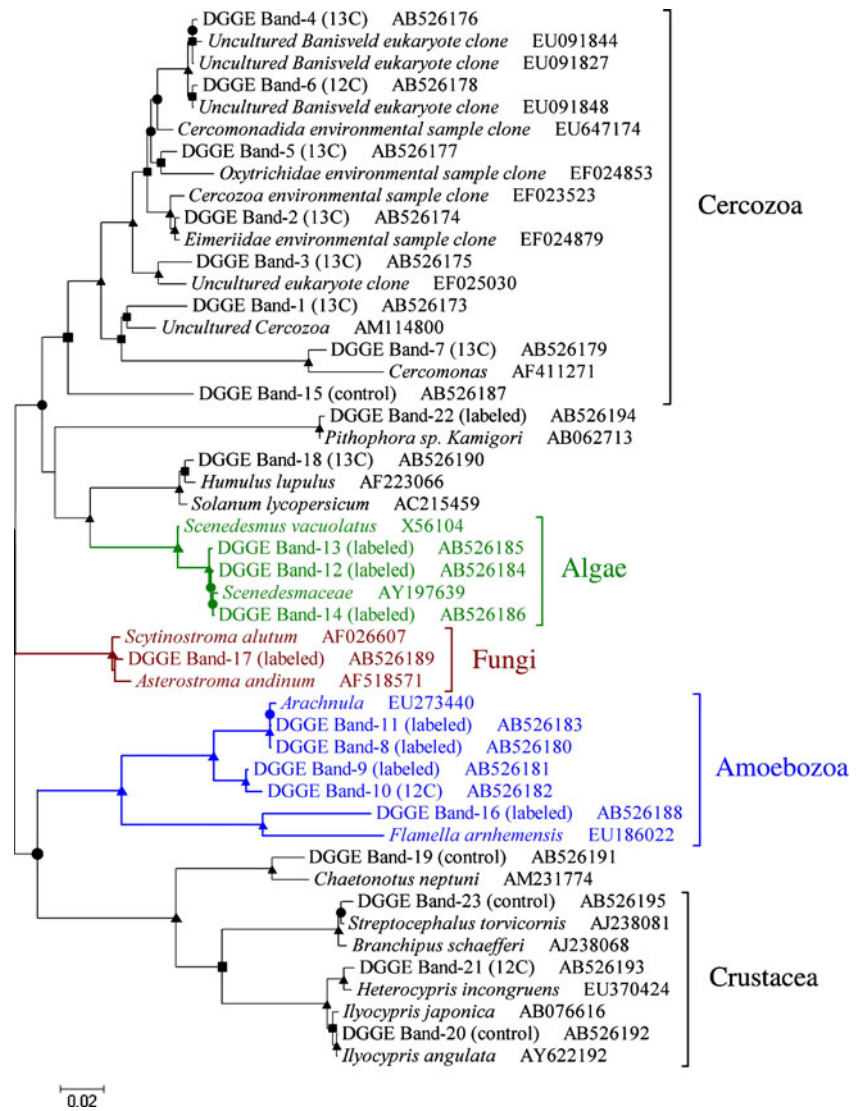
changes in bacterial and eukaryotic communities in paddy soil, when compared to those in the control without formate. A positive response to formate treatment was observed for bacteria affiliated with *A. transvaalensis* and *Firmicutes* bacteria, compared to a negative response for *Nitrospirae* bacteria. The underlying cause of these observations might be the selective grazing pressure of certain protozoa triggered by formate-based phototrophy (Rønn et al. 2002; Murase et al. 2006). In contrast, primary consumers of amoebae-like organisms dominated the eukaryotic community, and they can be affected by formate phototrophy to a much less extent (Fig. 6a). This might be attributed to the availability of their prey and little change in niche during formate-based phototrophy. Additionally, *Crustacea* protozoa actively assimilate methane-derived carbon in rice soil under darkness (Murase et al. 2006; Murase and Frenzel 2007). In this study, since DGGE bands 1 to 7 (see Fig. 6a, affiliated with *Cercozoa* group)

were only detected in "light" DNA fractions unanimously, we concluded that *Cercozoa* is isolated from phototrophy-based microbial loop.

At a fine resolution with individual microorganism identities, DNA-SIP analysis unequivocally leads to a conceptual model (see Fig. 1) for the phototrophy-driven microbial loop in paddy soil, on the basis of formate carbon metabolisms. It indicates that the microbes in a food network can be categorized into two groups. Primary producers (such as purple phototrophic bacteria, cyanobacteria, and algae) harvest light energy to assimilate organic or inorganic compounds, and consumers (including amoebozoa and fungi) grow on the biomass and/or metabolites of phototrophic microorganisms. They together form a complex microbial food web in the rice soil. This microbial food chain is distinct from methane-driven microbial loop in darkness (Murase and Frenzel 2007). In darkness, methane carbon in paddy soil is assimilated by soil

protozoa ranging from ciliate, flagellate, to amoeba. This observation implies that the predation relationship between protozoa and primary producing microorganisms is far more complicated in natural environment than in culture (Dillon and Parry 2009). In addition, the selective grazing pressure of certain protozoa on prey shapes the structure of bacterial populations in soils. This could further provoke more complicated carbon flux, such as the biomass decomposition of the aged eukaryotes (Hahn and Höfle 1998; Jürgens and Matz 2002). The elucidation of both top-down and bottom-up effects of organisms in sustaining the carbon and energy flow would be of great help toward a better understanding of soil productivity.

References

Achenbach LA, Carey J, Madigan MT (2001) Photosynthetic and phylogenetic primers for detection of anoxygenic phototrophs in natural environments. Appl Environ Microbiol 67:2922–2926

Al-Najjar MAA, de Beer D, Jorgensen BB, Kuhl M, Polerecky L (2010) Conversion and conservation of light energy in a photosynthetic microbial mat ecosystem. ISME J 4:440–449

Asari N, Ishihara R, Nakajima Y, Kimura M, Asakawa S (2008) Cyanobacterial communities of rice straw left on the soil surface of a paddy field. Biol Fertil Soils 44:605–612

Bass D, Chao EE-Y, Nikolaev S, Yabuki A, Ishida K-I, Berney C, Pakzad U, Wylezich C, Cavalier-Smith T (2009) Phylogeny of novel naked filose and reticulose Cercozoa: Granofilosea cl. n. and proteomyxidea revised. Protist 160:75–109

Baziramakenga R, Simard RR, Leroux GD (1995) Determination of organic acids in soil extracts by ion chromatography. Soil Biol Biochem 27:349–356

Beatriz D, Carlos P-A, Terence LM, Ramon M (2001) Application of denaturing gradient gel electrophoresis (DGGE) to study the diversity of marine picoeukaryotic assemblages and comparison of DGGE with other molecular techniques. Appl Environ Microbiol 67:2942–2951

Biddle JF, Fitz-Gibbon S, Schuster SC, Brenchley JE, House CH (2008) Metagenomic signatures of the Peru Margin subseafloor biosphere show a genetically distinct environment. Proc Natl Acad Sci USA 105:10583–10588

Cahyani VR, Matsuya K, Asakawa S, Kimura M (2004) Succession and phylogenetic profile of eukaryotic communities in the composting process of rice straw estimated by PCR-DGGE analysis. Biol Fertil Soils 40:334–344

Callieri C, Karjalainen SM, Passoni S (2002) Grazing by ciliates and heterotrophic nanoflagellates on picocyanobacteria in Lago Maggiore, Italy. J Plankton Res 24:785–796

Chauhan A, Cherrier J, Williams HN (2009) Impact of sideways and bottom-up control factors on bacterial community succession over a tidal cycle. Proc Natl Acad Sci USA 106:4301–4306

Deines P, Bodelier PLE, Eller G (2007) Methane-derived carbon flows through methane-oxidizing bacteria to higher trophic levels in aquatic systems. Environ Microbiol 9:1126–1134

Dillon A, Parry JD (2009) Amoebic grazing of freshwater Synechococcus strains rich in phycocyanin. FEMS Microbiol Ecol 69:106–112

Ding WX, Meng L, Yin YF, Cai ZC, Zheng XH (2007) CO$_2$ emission in an intensively cultivated loam as affected by long-term application of organic manure and nitrogen fertilizer. Soil Biol Biochem 39:669–679

Feng Y, Lin X, Wang Y, Zhang J, Mao T, Yin R, Zhu J (2009) Free-air CO$_2$ enrichment (FACE) enhances the biodiversity of purple phototrophic bacteria in flooded paddy soil. Plant Soil 324:317–328

Ferry JG (1990) Formate dehydrogenase. FEMS Microbiol Rev 87:377–382

Field CB, Behrenfeld MJ, Randerson JT, Falkowski P (1998) Primary production of the biosphere: integrating terrestrial and oceanic components. Science 281:237–240

Fujita Y, Nakahara H (2006) Variations in the microalgal structure in paddy soil in Osaka, Japan: comparison between surface and subsurface soils. Limnol 7:83–91

Haddock JD, Ferry JG (1989) Purification and properties of phloroglucinol reductase from Eubacterium oxidoreducens. J Boil Chem 264:4423–4427

Hahn MW, Höfle MG (1998) Grazing pressure by a bacterivorous flagellate reverses the relative abundance of Comamonas acidovorans PX54 and Vibrio strain CB5 in chemostat cocultures. Appl Environ Microbiol 64:1910–1918

Haque MZ, Kobayashi M, Fujii K, Takahashi E (1969) Seasonal changes of photosynthetic bacteria and their products. Soil Sci Plant Nutr 15:51–55

Harada N, Otsuka S, Nishiyama M, Matsumoto S (2003) Characteristics of phototrophic purple bacteria isolated from a Japanese paddy soil. Soil Sci Plant Nutr 49:521–526

Hatamoto M, Tanahashi T, Murase J, Matsuya K, Hayashi M, Kimura M, Asakawa S (2008) Eukaryotic communities associated with the decomposition of rice straw compost in a Japanese rice paddy field estimated by DGGE analysis. Biol Fertil Soils 44:527–532

Imhoff JF (1988) Anoxygenic phototrophic bacteria. Wiley, New York

Jia ZJ, Conrad R (2009) Bacteria rather than Archaea dominate microbial ammonia oxidation in an agricultural soil. Environ Microbiol 11:1658–1671

Jiao NZ, Zhang Y, Zeng YH, Hong N, Liu RL, Chen F, Wang PX (2007) Distinct distribution pattern of abundance and diversity of aerobic anoxygenic phototrophic bacteria in the global ocean. Environ Microbiol 9:3091–3099

Jürgens K, Matz C (2002) Predation as a shaping force for the phenotypic and genotypic composition of planktonic bacteria. Anton Leeuw Int J G 81:413–434

Kalyuzhnaya MG, Lapidus A, Ivanova N, Copeland AC, McHardy AC, Szeto E, Salamov A, Grigoriev IV, Suciu D, Levine SR, Markowitz VM, Rigoutsos I, Tringe SG, Bruce DC, Richardson PM, Lidstrom ME, Chistoserdova L (2008) High-resolution metagenomics targets specific functional types in complex microbial communities. Nat Biotechnol 26:1029–1034

Kimura M (2000) Anaerobic microbiology in waterlogged rice fields. Marcel Dekker, New York

Kudryavtsev A, Wylezich C, Schlegel M, Walochnik J, Michel R (2009) Ultrastructure, SSU rRNA gene sequences and phylogenetic relationships of Flamella Schaeffer, 1926 (Amoebozoa), with description of three new species. Protist 160:21–40

Lakshmi KVNS, Sasikala C, Ramana CV (2009) Rhodoplanes pokkaliisoli sp nov., a phototrophic alphaproteobacterium isolated from a waterlogged brackish paddy soil. Int J Syst Evol Microbiol 59:2153–2157

Liesack W, Schnell S, Revsbech NP (2000) Microbiology of flooded rice paddies. FEMS Microbiol Rev 24:625–645

Lueders T, Kindler R, Miltner A, Friedrich MW, Kaestner M (2006) Identification of bacterial micropredators distinctively active in a soil microbial food web. Appl Environ Microbiol 72:5342–5348

Madigan MT, Gest H (1979) Growth of the photosynthetic bacterium *Rhodopseudomonas capsulata* chemolithotrophically in darkness with H_2 as the energy source. J Bacteriol 137:524–530

Matsuguchi T, Yoo ID (1981) Stimulation of phototrophic N_2 fixation in paddy fields through rice straw application. Australian Academy of Science, Canberra

Moran MA, Miller WL (2007) Resourceful heterotrophs make the most of light in the coastal ocean. Nat Rev Microbiol 5:792–800

Murase J, Frenzel P (2007) A methane-driven microbial food web in a wetland rice soil. Environ Microbiol 9:3025–3034

Murase J, Noll M, Frenzel P (2006) Impact of protists on the activity and structure of the bacterial community in a rice field soil. Appl Environ Microbiol 72:5436–5444

Muyzer G, Brinkhoff T, Nübel U, Santegoeds C, Schäfer H, Wawer C (1998) Denaturing gradient gel electrophoresis (DGGE) in microbial ecology. Kluwer Academic, Dordrecht

Nagashima KVP, Hiraishi A, Shimada K, Matsuura K (1997) Horizontal transfer of genes coding for the photosynthetic reaction centers of purple bacteria. J Mol Evol 45:131–136

Neufeld JD, Dumont MG, Vorha J, Murrell JC (2007) Methodological considerations for the use of stable isotope probing in microbial ecology. Microb Ecol 53:435–442

Overmann J, Garcia-Pichel F (2006) The phototrophic way of life. Prokaryotes 2:32–85

Penning H, Conrad R (2006) Carbon isotope effects associated with mixed-acid fermentation of saccharides by Clostridium papyrosolvens. Geochim Cosmochim Acta 70:2283–2297

Pfennig N (1978) In: Clayton RK, Sistrom W (eds) General physiology and ecology of photosynthetic bacteria. Plenum, New York

Pickup ZL, Pickup R, Parry JD (2007) Growth of Acanthamoeba castellanii and Hartmannella vermiformis on live, heat-killed and DTAF-stained bacterial prey. FEMS Microbiol Ecol 61:264–272

Radajewski S, McDonald IR, Murrell JC (2003) Stable-isotope probing of nucleic acids: a window to the function of uncultured microorganisms. Curr Opin Biotechnol 14:296–302

Roeselers G, van Loosdrecht MCM, Muyzer G (2007) Heterotrophic pioneers facilitate phototrophic biofilm development. Microb Ecol 54:578–585

Rønn R, Mccaig AE, Griffiths BS, Prosser JI (2002) Impact of protozoan grazing on bacterial community structure in soil microcosms. Appl Environ Microbiol 68:6094–6105

Sugano A, Tsuchimoto H, Tun CC, Asakawa S, Kimura M (2007) Succession and phylogenetic profile of eukaryotic communities in rice straw incorporated into a rice field: estimation by PCR-DGGE and sequence analyses. Soil Sci Plant Nutr 53:585–594

Tamura K, Dudley J, Nei M, Kumar S (2007) MEGA4: Molecular Evolutionary Genetics Analysis (MEGA) software version 4.0. Mol Biol Evol 24:1596–1599

Tittel J, Bissinger V, Zippel B, Gaedke U, Bell E, Lorke A, Kamjunke N (2003) Mixotrophs combine resource use to outcompete specialists: implications for aquatic food webs. Proc Natl Acad Sci USA 100:12776–12781